Draft version July 4, 2025
Typeset using LaTeX **twocolumn** style in AASTeX7

Discovery and Preliminary Characterization of a Third Interstellar Object: 3I/ATLAS

Darryl Z. Seligman [1,*] Marco Micheli [2] Davide Farnocchia [3] Larry Denneau [4] John W. Noonan [5] Toni Santana-Ros [6,7] Luca Conversi [2] Maxime Devogèle [2] Laura Faggioli [2] Adina D. Feinstein [1,†] Marco Fenucci [2] Tessa Frincke [1] Olivier R. Hainaut [8] Willem B. Hoogendam [4,‡] Henry H. Hsieh [9] Theodore Kareta [10,11] Michael S. P. Kelley [12] Tim Lister [13] Dušan Marčeta [14] Karen J. Meech [4] Francisco Ocaña [2] Eloy Peña-Asensio [15] Benjamin J. Shappee [4] Aster G. Taylor [16,§] Richard Wainscoat [4] Robert Weryk [17] James J. Wray [18] Atsuhiro Yaginuma [19] Bin Yang [20] and Quanzhi Ye (叶泉志) [21,22]

[1] *Department of Physics and Astronomy, Michigan State University, East Lansing, MI 48824, USA*
[2] *ESA NEO Coordination Centre, Largo Galileo Galilei 1, I-00044 Frascati (RM), Italy*
[3] *Jet Propulsion Laboratory, California Institute of Technology, 4800 Oak Grove Dr., Pasadena, CA 91109, USA*
[4] *Institute for Astronomy, University of Hawaii, 2680 Woodlawn Drive, Honolulu, HI 96822, USA*
[5] *Department of Physics, Auburn University, Edmund C. Leach Science Center, Auburn, 36849, AL, USA*
[6] *Departamento de Física, Ingeniería de Sistemas y Teoría de la Señal, Universidad de Alicante, Carr. San Vicente del Raspeig, s/n, 03690 San Vicente del Raspeig, Alicante, Spain*
[7] *Institut de Ciències del Cosmos (ICCUB), Universitat de Barcelona (UB), c. Martí Franquès, 1, 08028 Barcelona, Catalonia, Spain*
[8] *European Southern Observatory, Karl-Schwarzschild-St. 2, 85748 Garching-bei-München, Germany*
[9] *Planetary Science Institute, 1700 East Fort Lowell Rd., Suite 106, Tucson, AZ 85719, USA*
[10] *Dept. of Astrophysics and Planetary Science, Villanova University, Villanova, PA, USA*
[11] *Lowell Observatory, Flagstaff, AZ, USA*
[12] *Department of Astronomy, University of Maryland, College Park, MD 20742-0001, USA*
[13] *Las Cumbres Observatory, 6740 Cortona Drive, Suite 102, Goleta, CA 93117, USA*
[14] *Department of Astronomy, Faculty of Mathematics, University of Belgrade, Serbia*
[15] *Department of Aerospace Science and Technology, Politecnico di Milano, Via La Masa 34, 20156 Milano, Italy*
[16] *Dept. of Astronomy, University of Michigan, Ann Arbor, MI 48109, USA*
[17] *Department of Physics and Astronomy, The University of Western Ontario, 1151 Richmond Street, London, ON N6A 3K7, Canada*
[18] *School of Earth and Atmospheric Sciences, Georgia Institute of Technology, 311 Ferst Drive, Atlanta, GA 30332, USA*
[19] *Dept. of Physics and Astronomy, Michigan State University, East Lansing, MI 48824, USA*
[20] *Instituto de Estudios Astrofísicos, Facultad de Ingeniería y Ciencias, Universidad Diego Portales, Santiago, Chile*
[21] *Department of Astronomy, University of Maryland, College Park, MD 20742, USA*
[22] *Center for Space Physics, Boston University, 725 Commonwealth Ave, Boston, MA 02215, USA*

ABSTRACT

We report initial observations aimed at the characterization of a third interstellar object candidate. This object, 3I/ATLAS—also C/2025 N1 (ATLAS)—, was discovered on 2025 July 1 UT and has an orbital eccentricity of $e \sim 6.2$, perihelion of $q \sim 1.35$ au, inclination of $\sim 175°$, and hyperbolic velocity of $V_\infty \sim 60$ km s^{-1}. 3I/ATLAS has an absolute magnitude of $H_V \sim 12$, which corresponds to a nuclear radius of ~ 10 km, assuming an asteroid-like albedo of $p \sim 0.05$. The discovery of this object implies a spatial number density of $n_0 \sim 10^{-3}$ au^{-3} for objects with radii greater than or equal to that of 3I/ATLAS. We report deep stacked images obtained using the Canada-France-Hawaii Telescope that display faint activity. Using images obtained from the Las Cumbres Observatory 0.36 m telescopes at Haleakala and the 2.0 m Faulkes Telescope North, we find a small light curve variation of less than 0.2 mag for the object over a ~ 29 h time span. The visible/near-infrared spectral slope of the object is red, comparable to 1I/'Oumuamua. The object will be observable until September 2025, unobservable near perihelion due to low solar elongation, and observable again in November. This limitation unfortunately prohibits detailed observations at perihelion when the activity of 3I/ATLAS is likely to peak. Based on the experience of 1I/'Oumuamua and 2I/Borisov, we ask the community

Email: dzs@msu.edu

to maintain a constant observational presence while possible with photometric, spectroscopic, and polarimetric methods. Such observational data would constrain the (i) light curve, (ii) onset and variation of activity, and (iii) nongravitational effects. It is essential that the community collaborate to rapidly and comprehensively characterize these properties of 3I/ATLAS.

Keywords: Asteroids (72) — Comets (280) —Meteors (1041) — Interstellar Objects (52)

1. INTRODUCTION

The first two interstellar objects identified traversing the inner Solar System, 1I/'Oumuamua (G. V. Williams et al. 2017) and 2I/Borisov (G. Borisov et al. 2019), were discovered in 2017 and 2019 respectively. It has been suggested that interstellar objects could have formed in a protostellar disk (E. Gaidos et al. 2017) or within a giant molecular cloud core (C.-H. Hsieh et al. 2021). Although there is little hope of identifying the home systems for a given interstellar object (T. Hallatt & P. Wiegert 2020), they provide the only opportunity to directly measure the properties of cometary bodies that formed outside of our solar system.

These first interstellar objects displayed divergent properties. For one, while 1I/'Oumuamua displayed no cometary tail (K. J. Meech et al. 2017; Q.-Z. Ye et al. 2017; D. Jewitt et al. 2017; D. E. Trilling et al. 2018), its trajectory implied a nongravitational acceleration at $\sim 30\sigma$ (M. Micheli et al. 2018). Meanwhile, 2I/Borisov displayed definitive outgassing and dust activity (D. Jewitt & J. Luu 2019; A. Fitzsimmons et al. 2019; B. T. Bolin et al. 2020; Q. Ye et al. 2020; A. J. McKay et al. 2020; P. Guzik et al. 2020; M.-T. Hui et al. 2020; Y. Kim et al. 2020; G. Cremonese et al. 2020; B. Yang et al. 2021). The excess velocity of 1I/'Oumuamua and 2I/Borisov also differed significantly. These objects had velocities of $V_\infty \sim 26$ km s^{-1} and $V_\infty \sim 32$ km s^{-1} respectively, which approximately correspond to ages of $\sim 10^2$ and $\sim 10^3$ Myr (E. Mamajek 2017; E. Gaidos et al. 2017; F. Feng & H. R. A. Jones 2018; F. Almeida-Fernandes & H. J. Rocha-Pinto 2018; T. Hallatt & P. Wiegert 2020; C.-H. Hsieh et al. 2021). In addition, 1I/'Oumuamua displayed brightness variations of ~ 3.5 magnitude corresponding to an extreme oblate $6:6:1$ geometry (M. Drahus et al. 2017; M. M. Knight et al. 2017; B. T. Bolin et al. 2018; W. C. Fraser et al. 2018; A. McNeill et al. 2018; M. J. S. Belton et al. 2018; S. Mashchenko 2019) and had a moderately red reflectance spectrum (J. Masiero 2017; A. Fitzsimmons et al. 2018; M. T. Bannister et al. 2017).

These divergent properties led to a variety of hypothesis regarding the provenance of the population. Although 2I/Borisov's coma displayed volatile species typically seen in comets (C. Opitom et al. 2019; T. Kareta et al. 2020; H. W. Lin et al. 2020; M. T. Bannister et al. 2020; Z. Xing et al. 2020; K. Aravind et al. 2021), it had a high enrichment of CO relative to H_2O (D. Bodewits et al. 2020; M. A. Cordiner et al. 2020). These ratios differentiate its composition from most solar system comets, which are typically rich in H_2O and contain CO between 1-15% relative to water (N. Biver et al. 2024).

1I/'Oumuamua's lack of cometary tail despite its nongravitational acceleration have led to a variety of hypothesized origins. M. Micheli et al. (2018) noted that for radiation pressure to cause the nongravitational acceleration, the object must either have an exceptionally low density or an extreme geometry. Such a density is a possible byproduct of diffusion-limited aggregation formation processes in the outskirts of a protostellar disk (A. Moro-Martín 2019). Somewhat counterintuitively, it has also been demonstrated that such hypothetical structures bound together by weak van der Waals forces could survive tidal disruption from Solar tides (E. G. Flekkøy et al. 2019). It was also hypothesized that such a fractal aggregate could form in the coma of a undiscovered parent interstellar comet (J. X. Luu et al. 2020).

Alternatively, 1I/'Oumuamua could have been outgassing volatiles with low levels of dust production, rendering it photometrically inactive in all extant observations (M. Micheli et al. 2018; Z. Sekanina 2019; D. Seligman & G. Laughlin 2020; W. G. Levine et al. 2021; W. G. Levine & G. Laughlin 2021; S. J. Desch & A. P. Jackson 2021; A. P. Jackson & S. J. Desch 2021; S. J. Desch & A. P. Jackson 2022; J. B. Bergner & D. Z. Seligman 2023). This argument has been recently bolstered; since the discovery of 1I/'Oumuamua, a series of photometrically inactive near-Earth objects (NEOs) have been reported to have significant comet-like nongravitational accelerations (D. Farnocchia et al. 2023; D. Z. Seligman et al. 2023, 2024). These objects imply that 1I/'Oumuamua-like nongravitational accelerations may be more common than previously thought. Regardless,

* NSF Astronomy and Astrophysics Postdoctoral Fellow
† NHFP Sagan Fellow
‡ NSF Graduate Research Fellow
§ Fannie and John Hertz Foundation Fellow

our understanding of interstellar objects is incomplete. See A. Fitzsimmons et al. (2023), D. Z. Seligman & A. Moro-Martín (2023), D. Jewitt & D. Z. Seligman (2023), and A. Moro-Martín (2022) for recent reviews on this topic.

In this paper we report early observations and analysis to help inform the planned observing programs over the next few months.

2. DISCOVERY AND HYPERBOLIC ORBIT CHARACTERIZATION

3I/ATLAS was discovered through the robotic observing schedule from ATLAS Chile on the evening of 2025 July 1 and given the internal designation A11pl3Z[23] (see Figure 1). The discovery tracklet was immediately submitted to the Minor Planet Center (MPC). Follow-up observations were then conducted by ATLAS in Hawaii, Sutherland (South Africa), and the Canary Islands, along with dozens of other observatories worldwide. The discovery was made by ATLAS largely because the object was located in the Galactic plane—a region typically avoided by more sensitive surveys such as Pan-STARRS and Catalina Sky Survey.

Prediscovery pairs and triplets were identified in ATLAS data from five days earlier by Sam Deen and later refined and re-submitted to the MPC by the ATLAS team. Additional precovery images were later found in ZTF survey data using the method described above. The object had remained quite faint until the end of May, when it reached magnitude $\sim$ 20. At the time of discovery in the ATLAS data, it had brightened to magnitude 17.7-17.8 in the o-band filter (see Figure 1).

This initial discovery and prediscovery arc, covering a total of about 18 days, is already sufficient to determine the large eccentricity, and consequently hyperbolic nature of the object's orbit. As soon as the unusual nature of the object became evident, a large amount of follow-up observations were obtained on 2025 July 2 by various observatories, leading to additional astrometric measurements, including those reported here (as better outlined below in Section 3).

Our best estimate of the heliocentric orbital elements of the object, at the time of posting of this paper, are listed in Table 1. In Figure 2, we show the orbit of the object in comparison to previously discovered interstellar objects.

From the current heliocentric orbit it is possible to infer the incoming trajectory of the object before it entered our Solar System. The eccentricity of the object's orbit with respect to the Solar System barycenter, computed before interacting with our planetary system, can be extrapolated as $e_b = 6.21 \pm 0.11$. This value, together with an incoming pericenter distance of $q_b = (1.371 \pm 0.014)$ au, results in an incoming velocity $v_\infty = (58 \pm 1)$ km s^{-1}, from an asymptote directed to-

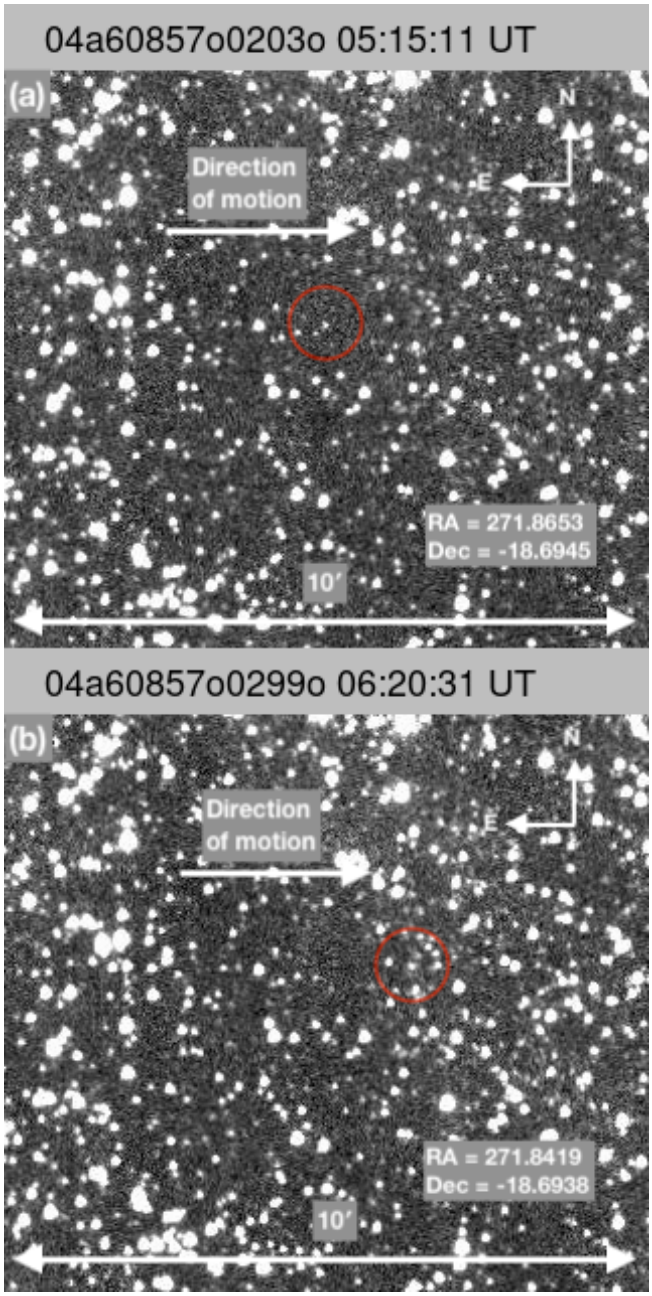

Figure 1. Cutout images from the first and fourth discovery observations of 3I/ATLAS from the ATLAS Chile, spanning approximately one hour. 3I/ATLAS is moving at 0.49 deg/day against the stellar background. The cardinal directions and direction of motion are indicated with arrows, and 3I/ATLAS identified within the red circle. (a) Unsubtracted image from 05:15:11 UT; (b) Unsubtracted image from 06:20:31 UT.

[23] https://www.minorplanetcenter.net/mpec/K25/K25N12.html

Table 1. Initial orbit of 3I/ATLAS, computed with 132 astrometric observations (three excluded as outliers) extending from 2025 June 14 to 2025 July 1. Heliocentric orbital elements at the epoch of 2025 July 1.0 TT.

Orbital element	Value ± 1σ
Perihelion distance q [au]	1.3655706 ± 0.0137087
Eccentricity e	6.202526 ± 0.104953
Inclination i [°]	175.11370 ± 0.00460
Longitude of ascending node Ω [°]	322.19723 ± 0.11135
Argument of perihelion ω [°]	127.88693 ± 0.14201
Time of perihelion T_P [MJD, TT]	60977.39531 ± 0.21759

wards a Right Ascension of $\sim 295°$ and a Declination of $\sim -19°$, in the constellation of Sagittarius and not far from the Galactic Center.

3. LIGHT CURVE AND ACTIVITY

As soon as the interstellar nature of the object became evident, we obtained observations with the European Space Agency's (ESA) Test Bed Telescopes (TBTs) and the Las Cumbres Observatory (LCO) telescopes, exploiting the ideal location of TBT in Chile and of the Haleakalā (Hawaii, USA) node of the LCO network.

We first tasked ESA's 0.56 m TBT (MPC code W57) at the La Silla Observatory (Chile). The telescope has a field of view of 2.5 × 2.5 degrees and is fully devoted to NEO survey and follow-up jobs. It can be interrupted at any time for these high-profile targets. We acquired 31 unfiltered 163 s exposures starting at 06:34 UT July 2 spanning a total of 93 minutes. Astrometry was reported in ADES format including astrometric uncertainties.

In parallel, we obtained detections with one of the 0.36 m telescopes on Haleakalā (MPC code T03), confirming the existence of the object and extracting some astrometric measurements with uncertainties of approximately ±0.″25. The measurements were immediately reported to the MPC in ADES format, including exposure-specific astrometric uncertainties.

We subsequently scheduled a one-hour observing sequence using two separate 0.36-meter telescopes from the LCO Haleakalā observatory (MPC codes T03, T04) and the 2.0 m Faulkes Telescope North (FTN, MPC code F65), part of the same network. The goal was to obtain a preliminary light curve and determine whether this newly detected object exhibited rotational variability as extreme as that observed in 1I/'Oumuamua. In contrast to the first known interstellar object, however, 3I/ATLAS displays a notably flat light curve with brightness variations of less than 0.2 magnitude over the observed 29-hour time span (see Figure 3). Additional follow-up observations will be necessary to constrain its

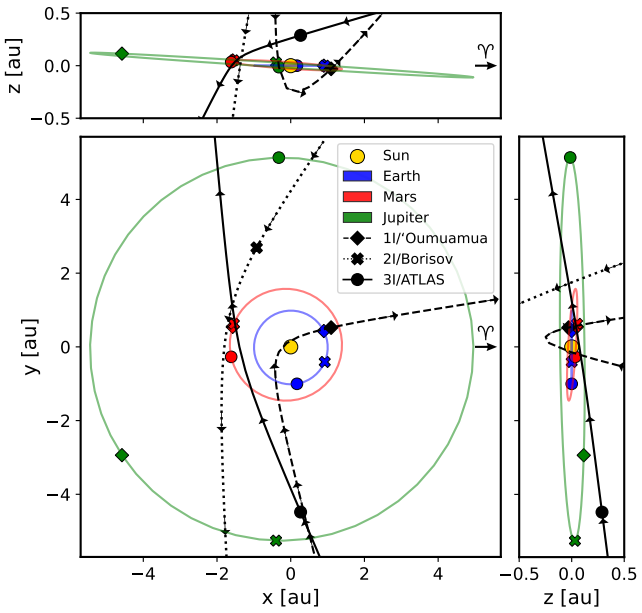

Figure 2. Heliocentric orbit (ECLIPJ2000) of 1I/'Oumuamua, 2I/Borisov, 3I/ATLAS (A11pl3Z), Earth, Mars, and Jupiter. Markers denote each body position at discovery. Vernal equinox direction is indicated.

rotation period. These images were also used to extract further astrometric measurements, accurate to approximately ±0.″1 (also already reported in ADES to the MPC), which provide a high-fidelity anchoring point to our orbital solution.

A series of 3 × 60 s *gri*-band non-sidereally guided images were obtained with the MegaCam mosaic-CCD on the 3.6 m Canada-France-Hawaii Telescope (CFHT; MPC code T14) on 2025 July 2 to check for faint cometary activity. The highest-quality image had a stellar FHWM of 0.″72±0.″05 measured perpendicular to the direction of trailing, while the object had a FWHM of 1.″29±0.″02. The magnitude in a 5.″ radius aperture was 17.2 in the *Gaia* DR2 G band after three background stars were masked, although the field was crowded. Figure 4 shows stacked composite image of these data in which faint activity is visible.

4. COLOR

We observed the target with the 2.0 m FTN on Haleakalā using the four-channel *MuSCAT3* imager, which records the Sloan g'-, r'-, i'-, and z_s-bands simultaneously. Two multi-filter imaging sequences were obtained: (i) six exposures of 30 s in each filter, and (ii) three exposures of 50 s in each filter, yielding total integrations of 180 s and 150 s per band, respectively. For context, as part of the LCO Outbursting Objects Key project (LOOK; T. Lister et al. 2022), we also obtained deep imaging observations with FTN on the

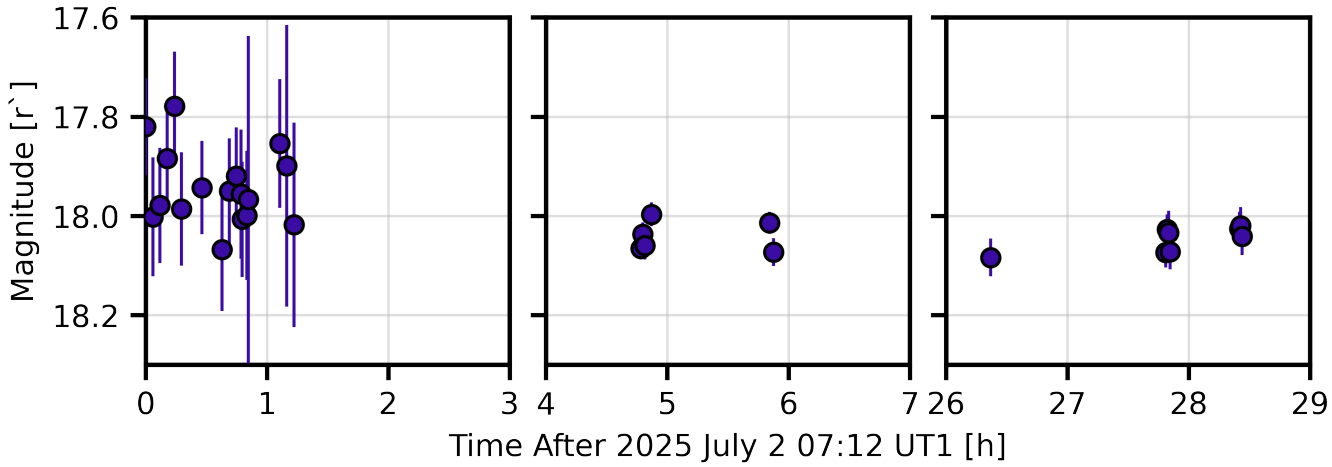

Figure 3. Light curve of 3I/ATLAS. The initial segment (left) was obtained with the Las Cumbres Observatory (LCO) 0.36 m telescopes at Haleakala (MPC code T03), while the middle and right segments were collected using the 2.0 m Faulkes Telescope North (FTN, MPC code F65). The data show a predominantly flat light curve, indicating minimal brightness variation during the observation period.

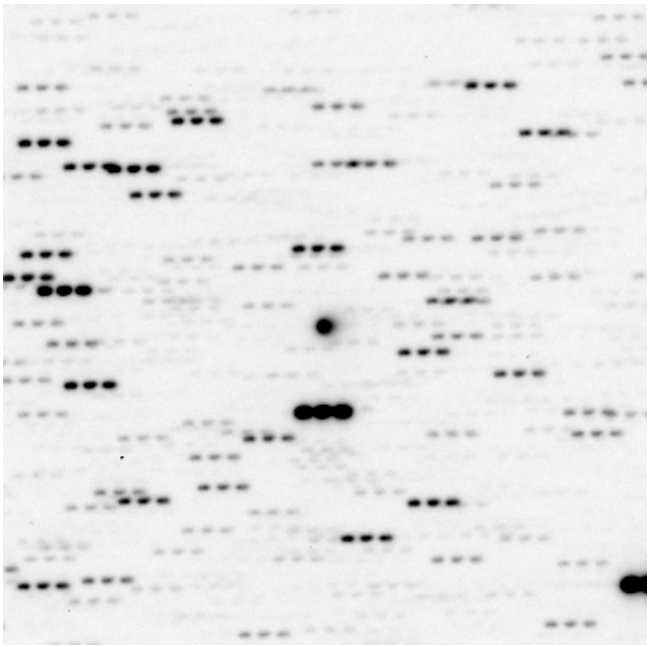

Figure 4. Stacked gri-band image cut-out (96″ width) from CFHT on 2025 July 2 showing faint activity. North is up, and East to the left.

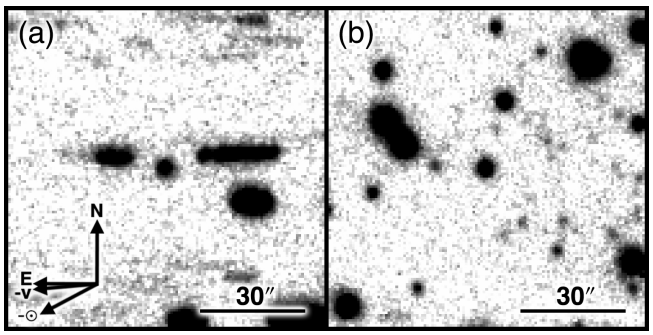

Figure 5. Stacked composite images of (a) 3I/ATLAS and (b) a reference field star constructed from 19 r'-band exposures of 60 s each (1140 s total integration time) using FTN on UT 2025 July 2.

same night to search for activity (and therefore judge the reliability of the multi-filter observations as being indicative of 3I/ATLAS's surface composition), where we found the target to be largely inactive (Figure 5). The data output by the LCO reduction pipelines were processed with PhotometryPipeline (M. Mommert 2017), which performs SCAMP astrometric solutions against *Gaia* DR3 and aperture photometry calibrated to Pan-STARRS DR2. In Figure 6, we show the resulting four-color surface reflectance spectrum of the object from the FTN.

We also utilized the 4.3 m Lowell Discovery Telescope (LDT) to observe as the object set on the morning of 2025 July 2 UT. Filtered images were taken sequentially (typically $r-g-i-r-z-r-z$) with the Large Monolithic Imager (LMI, P. Massey et al. 2013) in a 3 × 3 binning providing a per-pixel resolution of 0.″36. Cloud cover was highly variable but other atmospheric conditions were relatively stable, rendering the astrometry of several frames useful but the overall colors unreliable compared to those taken with FTN.

The colors of 3I/ATLAS as seen in Figure 6 are relatively linear (e.g., without obvious absorption features or spectral curvature) significantly redder than those of the Sun. This reflectance spectrum is similar to that retrieved for 1I/'Oumuamua by Q.-Z. Ye et al. (2017) and 2I/Borisov by J. de León et al. (2020), both slightly

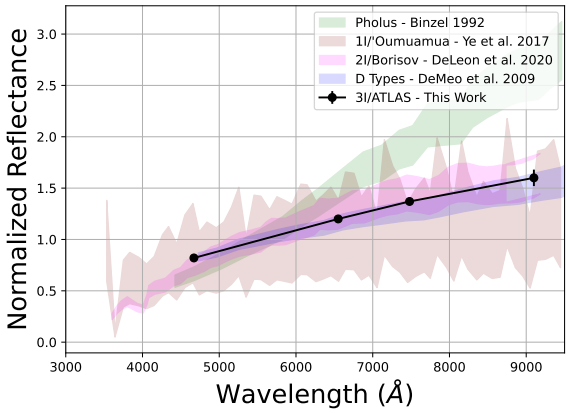

Figure 6. The g',r',i',z' colors of 3I/ATLAS obtained with FTN normalized at 5500 Å and plotted against 1I/'Oumuamua (Q.-Z. Ye et al. 2017), 2I/Borisov (J. de León et al. 2020), the extremely red Centaur Pholus (R. P. Binzel 1992), and the mean D-type asteroid spectrum (F. E. DeMeo et al. 2009). Note that errors on the color measurement are plotted, but are approximately the size of the plot points. 3I/ATLAS shows a moderately red spectral slope similar to 1I/'Oumuamua and 2I/Borisov.

redder than the D-type asteroids F. E. DeMeo et al. (2009), but not as red as seen in some outer Solar System objects. Given that 3I/ATLAS is at least weakly active, some of the reflected light must be from its coma – but cometary comae are only sometimes this red for typical dust compositions (see modeling and discussions of typical Solar System comets in S. Protopapa et al. 2018; T. Kareta et al. 2023). 2I/Borisov's coma was similarly red (see, e.g., J. de León et al. 2020), but the object was also significantly more active at the time of the observations. Depending on the size of 3I/ATLAS's nucleus, these reflected colors could indicate an underlying 1I/'Oumuamua-like surface with minimal dust contamination or a 2I/Borisov-like coma drowning out the nuclear signal. The flatness of 3I/ATLAS's lightcurve might indicative of the latter.

5. DISCUSSION

The lower-limit absolute magnitude of 3I/ATLAS is $H_V \sim 12$, assuming that the object is asteroid-like. For a given absolute magnitude, the size of an inactive object is given by (P. Pravec & A. W. Harris 2007):

$$R_{\rm Nuc} = \left(\frac{1329}{2\sqrt{p}}\right) 10^{-0.2\,H}\,. \tag{1}$$

In Equation 1, p is the geometric albedo, H is the absolute magnitude, and $R_{\rm Nuc}$ is the radius of the nucleus as measured in kilometers. Eq. 1 implies that the radius of 3I/ATLAS, $R_{\rm 3I}$, is:

$$R_{\rm 3I} = 11.8\,{\rm km}\left(\frac{0.05}{p}\right)^{-1/2} \tag{2}$$

This estimate assumes that 3I/ATLAS is asteroid-like; however as shown in Figure 4 there is coma present, so this represents an upper limit.

The discovery of 3I/ATLAS allows us to calculate a preliminary order of magnitude estimate of the number density of interstellar objects in its size range. For objects with a number density n, a velocity v_∞, and that are detected within a distance d, the detection rate $\Gamma = \pi d^2 v_\infty n$. ATLAS observes the entire night sky down to apparent magnitude 19 every night. We will assume that ATLAS has a 100% completeness for all objects with apparent magnitude $m \leq 19$ that appears in the night sky. For an object with an absolute magnitude of H, the apparent magnitude m is given by:

$$m = H + 5\log_{10}\left(\frac{d_S d_O}{\rm au^2}\right) - 2.5\log_{10} q(\alpha)\,. \tag{3}$$

Here, d_S is the distance from the object to the Sun, d_O is the distance from the object to the Earth, and $q(\alpha)$ is a function of the phase angle that accounts for opposition brightening. For simplicity, we will assume that the phase angle factor has an angle-averaged value of $q(\alpha) \sim 0.3$ and that $d = d_S = d_O$. With these approximations, ATLAS will discover all objects with an absolute magnitude of $H \leq 12$ that pass within a distance of $d = 4$ au. Since ground-based surveys like ATLAS survey only cover about two thirds of the sky and $v_\infty = 60$ km/s, the estimated detection rate of objects with $H \leq 12$ is:

$$\Gamma \simeq 300\ {\rm au^3/yr}\, n\,. \tag{4}$$

Since ATLAS has been monitoring the entire sky for three years and has found one interstellar object, the implied number density is $n \simeq 10^{-3}$ au^{-3}. We note that this is only an order-of-magnitude estimate. Regardless, this is much smaller than the estimated 0.1 au^{-3} calculated for 1I/'Oumuamua and 2I/Borisov.

It is immediately apparent that 3I/ATLAS is not in the same class of object as 1I/'Oumuamua or 2I/Borisov. Where 1I/'Oumuamua had a varying light curve (D. Jewitt & J. Luu 2019; A. Fitzsimmons et al. 2019; B. T. Bolin et al. 2020; Q. Ye et al. 2020; A. J. McKay et al. 2020; P. Guzik et al. 2020; M.-T. Hui et al. 2020; Y. Kim et al. 2020; G. Cremonese et al. 2020; B. Yang et al. 2021), 3I/ATLAS has little significant variation, but appears to have a similarly red slope (J. Masiero 2017; A. Fitzsimmons et al. 2018; M. T. Bannister et al. 2017). Whether this is due to similar natal

formation conditions or similar irradiation processes as an interstellar object is worthy of future investigation. In contrast to 2I/Borisov's significant cometary activity (D. Jewitt & J. Luu 2019; A. Fitzsimmons et al. 2019; B. T. Bolin et al. 2020; Q. Ye et al. 2020; A. J. McKay et al. 2020; P. Guzik et al. 2020; M.-T. Hui et al. 2020; Y. Kim et al. 2020; G. Cremonese et al. 2020; B. Yang et al. 2021), 3I/ATLAS shows only very weak activity. In addition, the newest interstellar object's apparent magnitude would make it likely an order of magnitude larger in size than 2I/Borisov. Therefore, 3I/ATLAS will probe a new size regime for the interstellar object size frequency distribution. All of these properties may change in the coming weeks as the object is heated for perhaps the first time during its perihelion passage. Comprehensive and collaborative investigations of 3I/ATLAS based off the lessons learned from the 1I/'Oumuamua and 2I/Borisov campaigns are poised to significantly expand our knowledge of the interstellar object population.

All of these data point to a clear action for the community — more observations across the spectrum are necessary. We encourage the observational astronomy community to collect data on 3I/ATLAS, be it photometry, spectroscopy, or polarimetry, to provide key evidence for the rotational phase light curve, any activity onset and variations, dust size frequency distributions, and constrain nongravitational acceleration. The perihelion of 3I/ATLAS will not be easily observable from Earth-based observatories, as the object will be on the opposite side of the Sun and at a low solar elongation angle. However, the object will approach within 0.4 au of Mars during perihelion, and we encourage nearby spacecraft (Mars Reconnaissance Orbiter, MAVEN, Jupiter Icy Moons Explorer) equipped with visible, UV, and IR spectrographs and cameras to capture data on this object's closest approach. Such data sets would be invaluable to understanding 3I/ATLAS's activity before and after its perihelion passage. Given the community's experience with 1I/'Oumuamua and 2I/Borisov, all observatories, instruments, and observational strategies are necessary to track any changes to the new interstellar object.

6. ACKNOWLEDGMENTS

D.Z.S. is supported by an NSF Astronomy and Astrophysics Postdoctoral Fellowship under award AST-2303553. This research award is partially funded by a generous gift of Charles Simonyi to the NSF Division of Astronomical Sciences. The award is made in recognition of significant contributions to Rubin Observatory' s Legacy Survey of Space and Time. D.F. conducted this research at the Jet Propulsion Laboratory, California Institute of Technology, under a contract with the National Aeronautics and Space Administration (80NM0018D0004). T.S-R. acknowledges funding from Ministerio de Ciencia e Innovaci ó n (Spanish Government), PGC2021, PID2021-125883NB-C21. This work was (partially) supported by the Spanish MICIN/AEI/10.13039/501100011033 and by "ERDF A way of making Europe" by the "European Union" through grant PID2021-122842OB-C21, and the Institute of Cosmos Sciences University of Barcelona (ICCUB, Unidad de Excelencia 'Marí a de Maeztu') through grant CEX2019-000918-M. A.D.F. acknowledges funding from NASA through the NASA Hubble Fellowship grant HST-HF2-51530.001-A awarded by STScI. A.G.T. acknowledges support from the Fannie and John Hertz Foundation and the University of Michigan's Rackham Merit Fellowship Program. E.P.-A. acknowledges support by the Italian Space Agency within the LUMIO project (ASI-PoliMi agreement n. 2024-6-HH.0). This material is based upon work supported by the National Science Foundation Graduate Research Fellowship Program under Grant Nos. 1842402 and 2236415. Any opinions, findings, conclusions, or recommendations expressed in this material are those of the author(s) and do not necessarily reflect the views of the National Science Foundation.

This research has made use of data and/or services provided by the International Astronomical Union's Minor Planet Center.

REFERENCES

Almeida-Fernandes, F., & Rocha-Pinto, H. J. 2018, A kinematical age for the interstellar object 1I/'Oumuamua, MNRAS, 480, 4903, doi: 10.1093/mnras/sty2202

Aravind, K., Ganesh, S., Venkataramani, K., et al. 2021, Activity of the first interstellar comet 2I/Borisov around perihelion: results from Indian observatories, MNRAS, 502, 3491, doi: 10.1093/mnras/stab084

Bannister, M. T., Schwamb, M. E., Fraser, W. C., et al. 2017, Col-OSSOS: Colors of the Interstellar Planetesimal 1I/'Oumuamua, ApJL, 851, L38, doi: 10.3847/2041-8213/aaa07c

Bannister, M. T., Opitom, C., Fitzsimmons, A., et al. 2020, Interstellar comet 2I/Borisov as seen by MUSE: C_2, NH_2 and red CN detections, arXiv e-prints, arXiv:2001.11605. https://arxiv.org/abs/2001.11605

Belton, M. J. S., Hainaut, O. R., Meech, K. J., et al. 2018, The Excited Spin State of 1I/2017 U1 Oumuamua, ApJL, 856, L21, doi: 10.3847/2041-8213/aab370

Bergner, J. B., & Seligman, D. Z. 2023, Acceleration of 1I/'Oumuamua from radiolytically produced H_2 in H_2O ice, Nature, 615, 610, doi: 10.1038/s41586-022-05687-w

Binzel, R. P. 1992, The optical spectrum of 5145 Pholus, Icarus, 99, 238, doi: 10.1016/0019-1035(92)90185-A

Biver, N., Dello Russo, N., Opitom, C., & Rubin, M. 2024, in Comets III, ed. K. J. Meech, M. R. Combi, D. Bockelée-Morvan, S. N. Raymodn, & M. E. Zolensky ( ), 459–498

Bodewits, D., Noonan, J. W., Feldman, P. D., et al. 2020, The carbon monoxide-rich interstellar comet 2I/Borisov, Nature Astronomy, 4, 867, doi: 10.1038/s41550-020-1095-2

Bolin, B. T., Weaver, H. A., Fernandez, Y. R., et al. 2018, APO Time-resolved Color Photometry of Highly Elongated Interstellar Object 1I/'Oumuamua, ApJL, 852, L2, doi: 10.3847/2041-8213/aaa0c9

Bolin, B. T., Lisse, C. M., Kasliwal, M. M., et al. 2020, Characterization of the Nucleus, Morphology, and Activity of Interstellar Comet 2I/Borisov by Optical and Near-infrared GROWTH, Apache Point, IRTF, ZTF, and Keck Observations, AJ, 160, 26, doi: 10.3847/1538-3881/ab9305

Borisov, G., Durig, D. T., Sato, H., et al. 2019, Comet C/2019 Q4 (Borisov), Central Bureau Electronic Telegrams, 4666, 1

Cordiner, M. A., Milam, S. N., Biver, N., et al. 2020, Unusually high CO abundance of the first active interstellar comet, Nature Astronomy, 4, 861, doi: 10.1038/s41550-020-1087-2

Cremonese, G., Fulle, M., Cambianica, P., et al. 2020, Dust Environment Model of the Interstellar Comet 2I/Borisov, ApJL, 893, L12, doi: 10.3847/2041-8213/ab8455

de León, J., Licandro, J., de la Fuente Marcos, C., et al. 2020, Visible and near-infrared observations of interstellar comet 2I/Borisov with the 10.4-m GTC and the 3.6-m TNG telescopes, MNRAS, 495, 2053, doi: 10.1093/mnras/staa1190

DeMeo, F. E., Binzel, R. P., Slivan, S. M., & Bus, S. J. 2009, An extension of the Bus asteroid taxonomy into the near-infrared, Icarus, 202, 160, doi: 10.1016/j.icarus.2009.02.005

Desch, S. J., & Jackson, A. P. 2021, 1I/ 'Oumuamua as an N2 ice fragment of an exo-pluto surface II: Generation of N2 ice fragments and the origin of 'Oumuamua, Journal of Geophysical Research: Planets, e2020JE006807

Desch, S. J., & Jackson, A. P. 2022, Some Pertinent Issues for Interstellar Panspermia Raised after the Discovery of 1I/'Oumuamua, Astrobiology, 22, 1400, doi: 10.1089/ast.2021.0199

Drahus, M., Yang, B., Lis, D. C., & Jewitt, D. 2017, New Limits to CO Outgassing in Centaurs, MNRAS, 468, 2897, doi: 10.1093/mnras/stw2227

Farnocchia, D., Seligman, D. Z., Granvik, M., et al. 2023, (523599) 2003 RM: The Asteroid that Wanted to be a Comet, PSJ, 4, 29, doi: 10.3847/PSJ/acb25b

Feng, F., & Jones, H. R. A. 2018, 'Oumuamua as a Messenger from the Local Association, ApJL, 852, L27, doi: 10.3847/2041-8213/aaa404

Fitzsimmons, A., Meech, K., Matrà, L., & Pfalzner, S. 2023, Interstellar Objects and Exocomets, arXiv e-prints, arXiv:2303.17980, doi: 10.48550/arXiv.2303.17980

Fitzsimmons, A., Snodgrass, C., Rozitis, B., et al. 2018, Spectroscopy and thermal modelling of the first interstellar object 1I/2017 U1 'Oumuamua, Nature Astronomy, 2, 133, doi: 10.1038/s41550-017-0361-4

Fitzsimmons, A., Hainaut, O., Meech, K. J., et al. 2019, Detection of CN Gas in Interstellar Object 2I/Borisov, ApJL, 885, L9, doi: 10.3847/2041-8213/ab49fc

Flekkøy, E. G., Luu, J., & Toussaint, R. 2019, The Interstellar Object 'Oumuamua as a Fractal Dust Aggregate, ApJL, 885, L41, doi: 10.3847/2041-8213/ab4f78

Fraser, W. C., Pravec, P., Fitzsimmons, A., et al. 2018, The tumbling rotational state of 1I/'Oumuamua, Nature Astronomy, 2, 383, doi: 10.1038/s41550-018-0398-z

Gaidos, E., Williams, J., & Kraus, A. 2017, Origin of Interstellar Object A/2017 U1 in a Nearby Young Stellar Association?, RNAAS, 1, 13, doi: 10.3847/2515-5172/aa9851

Guzik, P., Drahus, M., Rusek, K., et al. 2020, Initial characterization of interstellar comet 2I/Borisov, Nature Astronomy, 4, 53, doi: 10.1038/s41550-019-0931-8

Hallatt, T., & Wiegert, P. 2020, The Dynamics of Interstellar Asteroids and Comets within the Galaxy: An Assessment of Local Candidate Source Regions for 1I/' Oumuamua and 2I/Borisov, AJ, 159, 147

Hsieh, C.-H., Laughlin, G., & Arce, H. G. 2021, Evidence Suggesting That 'Oumuamua Is the 30 Myr Old Product of a Molecular Cloud, ApJ, 917, 20, doi: 10.3847/1538-4357/ac0729

Hui, M.-T., Ye, Q.-Z., Föhring, D., Hung, D., & Tholen, D. J. 2020, Physical Characterization of Interstellar Comet 2I/2019 Q4 (Borisov), AJ, 160, 92, doi: 10.3847/1538-3881/ab9df8

Jackson, A. P., & Desch, S. J. 2021, 1I/ 'Oumuamua as an N2 ice fragment of an exo-Pluto surface: I. Size and Compositional Constraints, Journal of Geophysical Research: Planets, e2020JE006706

Jewitt, D., & Luu, J. 2019, Initial Characterization of Interstellar Comet 2I/2019 Q4 (Borisov), ApJL, 886, L29, doi: 10.3847/2041-8213/ab530b

Jewitt, D., Luu, J., Rajagopal, J., et al. 2017, Interstellar Interloper 1I/2017 U1: Observations from the NOT and WIYN Telescopes, ApJL, 850, L36, doi: 10.3847/2041-8213/aa9b2f

Jewitt, D., & Seligman, D. Z. 2023, The Interstellar Interlopers, ARA&A, 61, 197, doi: 10.1146/annurev-astro-071221-054221

Kareta, T., Noonan, J. W., Harris, W. M., & Springmann, A. 2023, Ice, Ice, Maybe? Investigating 46P/Wirtanen's Inner Coma for Icy Grains, PSJ, 4, 85, doi: 10.3847/PSJ/accc28

Kareta, T., Andrews, J., Noonan, J. W., et al. 2020, Carbon Chain Depletion of 2I/Borisov, ApJL, 889, L38, doi: 10.3847/2041-8213/ab6a08

Kim, Y., Jewitt, D., Mutchler, M., et al. 2020, Coma Anisotropy and the Rotation Pole of Interstellar Comet 2I/Borisov, ApJL, 895, L34, doi: 10.3847/2041-8213/ab9228

Knight, M. M., Protopapa, S., Kelley, M. S. P., et al. 2017, On the Rotation Period and Shape of the Hyperbolic Asteroid 1I/'Oumuamua (2017 U1) from Its Lightcurve, ApJL, 851, L31, doi: 10.3847/2041-8213/aa9d81

Levine, W. G., Cabot, S. H. C., Seligman, D., & Laughlin, G. 2021, Constraints on the Occurrence of 'Oumuamua-Like Objects, ApJ, 922, 39, doi: 10.3847/1538-4357/ac1fe6

Levine, W. G., & Laughlin, G. 2021, Assessing the Formation of Solid Hydrogen Objects in Starless Molecular Cloud Cores, ApJ, 912, 3, doi: 10.3847/1538-4357/abec85

Lin, H. W., Lee, C.-H., Gerdes, D. W., et al. 2020, Detection of Diatomic Carbon in 2I/Borisov, ApJL, 889, L30, doi: 10.3847/2041-8213/ab6bd9

Lister, T., Kelley, M. S. P., Holt, C. E., et al. 2022, The LCO Outbursting Objects Key Project: Overview and Year 1 Status, PSJ, 3, 173, doi: 10.3847/PSJ/ac7a31

Luu, J. X., Flekkøy, E. G., & Toussaint, R. 2020, 'Oumuamua as a Cometary Fractal Aggregate: The "Dust Bunny" Model, ApJL, 900, L22, doi: 10.3847/2041-8213/abafa7

Mamajek, E. 2017, Kinematics of the Interstellar Vagabond 1I/Oumuamua (A/2017 U1), Research Notes of the American Astronomical Society, 1, 21, doi: 10.3847/2515-5172/aa9bdc

Mashchenko, S. 2019, Modelling the light curve of 'Oumuamua: evidence for torque and disc-like shape, MNRAS, 489, 3003, doi: 10.1093/mnras/stz2380

Masiero, J. 2017, Palomar Optical Spectrum of Hyperbolic Near-Earth Object A/2017 U1, arXiv e-prints, arXiv:1710.09977. https://arxiv.org/abs/1710.09977

Massey, P., Dunham, E. W., Bida, T. A., et al. 2013, in American Astronomical Society Meeting Abstracts, Vol. 221, American Astronomical Society Meeting Abstracts #221, 345.02

McKay, A. J., Cochran, A. L., Dello Russo, N., & DiSanti, M. A. 2020, Detection of a Water Tracer in Interstellar Comet 2I/Borisov, ApJL, 889, L10, doi: 10.3847/2041-8213/ab64ed

McNeill, A., Trilling, D. E., & Mommert, M. 2018, Constraints on the Density and Internal Strength of 1I/Oumuamua, ApJL, 857, L1, doi: 10.3847/2041-8213/aab9ab

Meech, K. J., Weryk, R., Micheli, M., et al. 2017, A brief visit from a red and extremely elongated interstellar asteroid, Nature, 552, 378, doi: 10.1038/nature25020

Micheli, M., Farnocchia, D., Meech, K. J., et al. 2018, Non-gravitational acceleration in the trajectory of 1I/2017 U1 ('Oumuamua), Nature, 559, 223, doi: 10.1038/s41586-018-0254-4

Mommert, M. 2017, PHOTOMETRYPIPELINE: An automated pipeline for calibrated photometry, Astronomy and Computing, 18, 47

Moro-Martín, A. 2019, Could 1I/' Oumuamua be an Icy Fractal Aggregate? ApJL, 872, L32

Moro-Martín, A. 2022, Interstellar planetesimals, arXiv e-prints, arXiv:2205.04277, doi: 10.48550/arXiv.2205.04277

Opitom, C., Fitzsimmons, A., Jehin, E., et al. 2019, 2I/Borisov: A C_2-depleted interstellar comet, A&A, 631, L8, doi: 10.1051/0004-6361/201936959

Pravec, P., & Harris, A. W. 2007, Binary asteroid population. 1. Angular momentum content, Icarus, 190, 250, doi: 10.1016/j.icarus.2007.02.023

Protopapa, S., Kelley, M. S. P., Yang, B., et al. 2018, Icy Grains from the Nucleus of Comet C/2013 US_{10} (Catalina), ApJL, 862, L16, doi: 10.3847/2041-8213/aad33b

Sekanina, Z. 2019, Outgassing As Trigger of 1I/'Oumuamua's Nongravitational Acceleration: Could This Hypothesis Work at All?, arXiv e-prints, arXiv:1905.00935. https://arxiv.org/abs/1905.00935

Seligman, D., & Laughlin, G. 2020, Evidence that 1I/2017 U1 ('Oumuamua) was Composed of Molecular Hydrogen Ice, ApJL, 896, L8, doi: 10.3847/2041-8213/ab963f

Seligman, D. Z., & Moro-Martín, A. 2023, Interstellar objects, Contemporary Physics, 63, 200, doi: 10.1080/00107514.2023.2203976

Seligman, D. Z., Farnocchia, D., Micheli, M., et al. 2023, Dark Comets? Unexpectedly Large Nongravitational Accelerations on a Sample of Small Asteroids, PSJ, 4, 35, doi: 10.3847/PSJ/acb697

Seligman, D. Z., Farnocchia, D., Micheli, M., et al. 2024, Two distinct populations of dark comets delineated by orbits and sizes, Proceedings of the National Academy of Science, 121, e2406424121, doi: 10.1073/pnas.2406424121

Trilling, D. E., Mommert, M., Hora, J. L., et al. 2018, Spitzer observations of interstellar object 1I/ ʻOumuamua, AJ, 156, 261

Williams, G. V., Sato, H., Sarneczky, K., et al. 2017, Minor Planets 2017 SN_33 and 2017 U1, Central Bureau Electronic Telegrams, 4450, 1

Xing, Z., Bodewits, D., Noonan, J., & Bannister, M. T. 2020, Water Production Rates and Activity of Interstellar Comet 2I/Borisov, ApJL, 893, L48, doi: 10.3847/2041-8213/ab86be

Yang, B., Li, A., Cordiner, M. A., et al. 2021, Compact pebbles and the evolution of volatiles in the interstellar comet 2I/Borisov, Nature Astronomy, doi: 10.1038/s41550-021-01336-w

Ye, Q., Kelley, M. S. P., Bolin, B. T., et al. 2020, Pre-discovery Activity of New Interstellar Comet 2I/Borisov beyond 5 au, AJ, 159, 77, doi: 10.3847/1538-3881/ab659b

Ye, Q.-Z., Zhang, Q., Kelley, M. S. P., & Brown, P. G. 2017, 1I/2017 U1 (ʻOumuamua) is Hot: Imaging, Spectroscopy, and Search of Meteor Activity, ApJL, 851, L5, doi: 10.3847/2041-8213/aa9a34